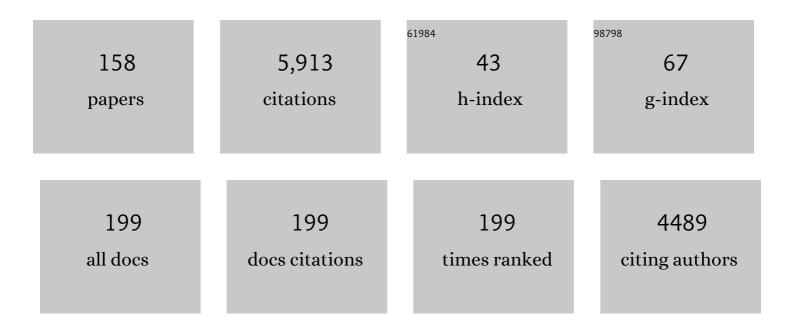
Thomas R Walter

List of Publications by Year in descending order

Source: https://exaly.com/author-pdf/7145536/publications.pdf Version: 2024-02-01



THOMAS P WAITED

| # | Article | IF | CITATIONS |
|----|--|------|-----------|
| 1 | Hidden mechanical weaknesses within lava domes provided by buried high-porosity hydrothermal alteration zones. Scientific Reports, 2022, 12, 3202. | 3.3 | 19 |
| 2 | Radar Scenario Generation for Automotive Applications in the E Band. IEEE Journal of Microwaves, 2022, 2, 253-261. | 6.5 | 3 |
| 3 | Cyclical geothermal unrest as a precursor to Iceland's 2021 Fagradalsfjall eruption. Nature Geoscience, 2022, 15, 397-404. | 12.9 | 29 |
| 4 | Volcanotectonics: the tectonics and physics of volcanoes and their eruption mechanics. Bulletin of Volcanology, 2022, 84, . | 3.0 | 7 |
| 5 | Automatic Detection of Volcanic Unrest Using Blind Source Separation With a Minimum Spanning Tree Based Stability Analysis. IEEE Journal of Selected Topics in Applied Earth Observations and Remote Sensing, 2021, 14, 7771-7787. | 4.9 | 7 |
| 6 | Anatomy of the Bezymianny volcano merely before an explosive eruption on 20.12.2017. Scientific Reports, 2021, 11, 1758. | 3.3 | 19 |
| 7 | A review framework of how earthquakes trigger volcanic eruptions. Nature Communications, 2021, 12, 1004. | 12.8 | 50 |
| 8 | A decade-long silent ground subsidence hazard culminating in a metropolitan disaster in Maceió, Brazil. Scientific Reports, 2021, 11, 7704. | 3.3 | 15 |
| 9 | Eruptive Cycle and Bubble Trap of Strokkur Geyser, Iceland. Journal of Geophysical Research: Solid Earth, 2021, 126, e2020JB020769. | 3.4 | 14 |
| 10 | Surveying fumarole sites and hydrothermal alteration by unoccupied aircraft systems (UAS) at the La Fossa cone, Vulcano Island (Italy). Journal of Volcanology and Geothermal Research, 2021, 413, 107208. | 2.1 | 14 |
| 11 | Constructive and Destructive Processes During the 2018–2019 Eruption Episode at Shiveluch Volcano, Kamchatka, Studied From Satellite and Aerial Data. Frontiers in Earth Science, 2021, 9, . | 1.8 | 8 |
| 12 | Thermal remote sensing reveals communication between volcanoes of the Klyuchevskoy Volcanic Group. Scientific Reports, 2021, 11, 13090. | 3.3 | 13 |
| 13 | A Radar Target Simulator for Generating Synthesised and Measured micro-Doppler-Signatures of Vulnerable Road Users. , 2021, , . | | 1 |
| 14 | Inflating Shallow Plumbing System of Bezymianny Volcano, Kamchatka, Studied by InSAR and Seismicity Data Prior to the 20 December 2017 Eruption. Frontiers in Earth Science, 2021, 9, . | 1.8 | 3 |
| 15 | Underwater and drone based photogrammetry reveals structural control at Geysir geothermal field in Iceland. Journal of Volcanology and Geothermal Research, 2020, 391, 106282. | 2.1 | 59 |
| 16 | Eruption Interval Monitoring at Strokkur Geyser, Iceland. Geophysical Research Letters, 2020, 47, e2019GL085266. | 4.0 | 18 |
| 17 | Insights into lava dome and spine extrusion using analogue sandbox experiments. Earth and Planetary Science Letters, 2020, 551, 116571. | 4.4 | 8 |
| 18 | The rebirth and evolution of Bezymianny volcano, Kamchatka after the 1956 sector collapse. Communications Earth & Environment, 2020, 1, . | 6.8 | 17 |

| # | Article | IF | CITATIONS |
|----|--|------|-----------|
| 19 | The 29 March 2017 Yuzhno-Ozernovskoe Kamchatka Earthquake: Fault Activity in An Extension of the East Kamchatka Fault Zone as Constrained by InSAR Observations. Bulletin of the Seismological Society of America, 2020, 110, 1101-1114. | 2.3 | 0 |
| 20 | UAS-based tracking of the Santiaguito Lava Dome, Guatemala. Scientific Reports, 2020, 10, 8644. | 3.3 | 24 |
| 21 | The 2019 Eruption Dynamics and Morphology at Ebeko Volcano Monitored by Unoccupied Aircraft Systems (UAS) and Field Stations. Remote Sensing, 2020, 12, 1961. | 4.0 | 18 |
| 22 | Processes culminating in the 2015Âphreatic explosion at Lascar volcano, Chile, evidenced by multiparametric data. Natural Hazards and Earth System Sciences, 2020, 20, 377-397. | 3.6 | 14 |
| 23 | Volcanological applications of unoccupied aircraft systems (UAS): Developments, strategies, and future challenges. Volcanica, 2020, 3, 67-114. | 1.8 | 63 |
| 24 | A Near-Range Radar Target Simulator for Automotive Radar Generating Targets of Vulnerable Road Users. IEEE Microwave and Wireless Components Letters, 2020, 30, 1213-1216. | 3.2 | 19 |
| 25 | Towards Global Volcano Monitoring Using Multisensor Sentinel Missions and Artificial Intelligence: The MOUNTS Monitoring System. Remote Sensing, 2019, 11, 1528. | 4.0 | 97 |
| 26 | Seismic activity during the 2013–2015 intereruptive phase at Lascar volcano, Chile. Geophysical Journal International, 2019, 219, 449-463. | 2.4 | 7 |
| 27 | Growth and collapse of a littoral lava dome during the 2018/19 eruption of Kadovar Volcano, Papua New Guinea, analyzed by multi-sensor satellite imagery. Journal of Volcanology and Geothermal Research, 2019, 388, 106704. | 2.1 | 19 |
| 28 | Hydrothermal alteration of andesitic lava domes can lead to explosive volcanic behaviour. Nature Communications, 2019, 10, 5063. | 12.8 | 76 |
| 29 | The impact of unloading stresses on post-caldera magma intrusions. Earth and Planetary Science Letters, 2019, 508, 109-121. | 4.4 | 13 |
| 30 | Load Stress Controls on Directional Lava Dome Growth at Volcán de Colima, Mexico. Frontiers in Earth Science, 2019, 7, . | 1.8 | 15 |
| 31 | Complex hazard cascade culminating in the Anak Krakatau sector collapse. Nature Communications, 2019, 10, 4339. | 12.8 | 105 |
| 32 | Unrest at Domuyo Volcano, Argentina, Detected by Geophysical and Geodetic Data and Morphometric Analysis. Remote Sensing, 2019, 11, 2175. | 4.0 | 17 |
| 33 | Deformations and Morphology Changes Associated with the 2016–2017 Eruption Sequence at Bezymianny Volcano, Kamchatka. Remote Sensing, 2019, 11, 1278. | 4.0 | 20 |
| 34 | A Radar Target Simulator Concept for Close-Range Targets with Micro-Doppler Signatures. , 2019, , . | | 6 |
| 35 | Volcanic activities triggered or inhibited by resonance of volcanic edifices to large earthquakes. Geology, 2019, 47, 67-70. | 4.4 | 16 |
| 36 | Slip Rate Variation Along the Kunlun Fault (Tibet): Results From New GPS Observations and a Viscoelastic Earthquake ycle Deformation Model. Geophysical Research Letters, 2019, 46, 2524-2533. | 4.0 | 45 |

| # | Article | IF | CITATIONS |
|----|--|------|-----------|
| 37 | Sinkholes and uvalas in evaporite karst: spatio-temporal development with links to base-level fall on the eastern shore of the Dead Sea. Solid Earth, 2019, 10, 1451-1468. | 2.8 | 22 |
| 38 | Imaging the 2013 explosive crater excavation and new dome formation at Volcán de Colima with TerraSAR-X, time-lapse cameras and modelling. Journal of Volcanology and Geothermal Research, 2019, 369, 224-237. | 2.1 | 23 |
| 39 | Morphological and structural changes at the Merapi lava dome monitored in 2012–15 using unmanned aerial vehicles (UAVs). Journal of Volcanology and Geothermal Research, 2018, 349, 256-267. | 2.1 | 68 |
| 40 | Structural weakening of the Merapi dome identified by drone photogrammetry after the 2010 eruption. Natural Hazards and Earth System Sciences, 2018, 18, 3267-3281. | 3.6 | 20 |
| 41 | The Relationship Between Lava Fountaining and Vent Morphology for the 2014–2015 Holuhraun Eruption, Iceland, Analyzed by Video Monitoring and Topographic Mapping. Frontiers in Earth Science, 2018, 6, . | 1.8 | 16 |
| 42 | Accelerated Aging of Cu(In,Ga)Se <inf>2</inf> Solar Cells under Dark Anneal and Electrical Bias Conditions. , 2018, , . | | 0 |
| 43 | Radar Path Delay Effects in Volcanic Gas Plumes: The Case of LÃ _i scar Volcano, Northern Chile. Remote Sensing, 2018, 10, 1514. | 4.0 | 12 |
| 44 | Fault behavior and lower crustal rheology inferred from the first seven years of postseismic GPS data after the 2008 Wenchuan earthquake. Earth and Planetary Science Letters, 2018, 495, 202-212. | 4.4 | 53 |
| 45 | Growth of a Volcanic Edifice Through Plumbing System Processes—Volcanic Rift Zones, Magmatic Sheet-Intrusion Swarms and Long-Lived Conduits. , 2018, , 89-112. | | 10 |
| 46 | Localized and distributed erosion triggered by the 2015 Hurricane Patricia investigated by repeated drone surveys and time lapse cameras at Volcán de Colima, Mexico. Geomorphology, 2018, 319, 186-198. | 2.6 | 21 |
| 47 | Constraints on the geomorphological evolution of the nested summit craters of Láscar volcano from high spatio-temporal resolution TerraSAR-X interferometry. Bulletin of Volcanology, 2018, 80, 1. | 3.0 | 10 |
| 48 | REFIR- A multi-parameter system for near real-time estimates of plume-height and mass eruption rate during explosive eruptions. Journal of Volcanology and Geothermal Research, 2018, 360, 61-83. | 2.1 | 15 |
| 49 | Video monitoring reveals pulsating vents and propagation path of fissure eruption during the March 2011 Pu'u 'Ō'ŕeruption, Kilauea volcano. Journal of Volcanology and Geothermal Research, 2017, 330, 43-55. | 2.1 | 17 |
| 50 | Sinkholes, subsidence and subrosion on the eastern shore of the DeadÂSea as revealed by a close-range photogrammetric survey. Geomorphology, 2017, 285, 305-324. | 2.6 | 57 |
| 51 | Multiple coincident eruptive seismic tremor sources during the 2014–2015 eruption at Holuhraun, Iceland. Journal of Geophysical Research: Solid Earth, 2017, 122, 2972-2987. | 3.4 | 27 |
| 52 | Thermal and gas dynamic investigations at Lastarria volcano, Northern Chile. The influence of precipitation and atmospheric pressure on the fumarole temperature and the gas velocity. Journal of Volcanology and Geothermal Research, 2017, 346, 134-140. | 2.1 | 13 |
| 53 | Evaluating links between deformation, topography and surface temperature at volcanic domes: Results from a multi-sensor study at VolcAin de Colima, Mexico. Earth and Planetary Science Letters, 2017, 479, 354-365. | 4.4 | 25 |
| 54 | The effect of giant lateral collapses on magma pathways and the location of volcanism. Nature Communications, 2017, 8, 1097. | 12.8 | 72 |

| # | Article | IF | CITATIONS |
|----|---|------|-----------|
| 55 | Effects of Host-rock Fracturing on Elastic-deformation Source Models of Volcano Deflation. Scientific Reports, 2017, 7, 10970. | 3.3 | 30 |
| 56 | Compound dislocation models (CDMs) for volcano deformation analyses. Geophysical Journal International, 2017, 208, 877-894. | 2.4 | 61 |
| 57 | Geomorphology and structural development of the nested summit crater of LÃ _i scar Volcano studied with Terrestrial Laser Scanner data and analogue modelling. Journal of Volcanology and Geothermal Research, 2017, 329, 1-12. | 2.1 | 12 |
| 58 | Significant lateral dip changes may have limited the scale of the 2015 <i>M</i> _{<i>w</i>} 7.8 Gorkha earthquake. Geophysical Research Letters, 2017, 44, 8847-8856. | 4.0 | 22 |
| 59 | Time-domain correlation radar for fluid surface velocity estimation using a 77 GHz sensor platform. , 2017, , . | | 13 |
| 60 | High-Resolution Digital Elevation Modeling from TLS and UAV Campaign Reveals Structural Complexity at the 2014/2015 Holuhraun Eruption Site, Iceland. Frontiers in Earth Science, 2017, 5, . | 1.8 | 37 |
| 61 | InSAR observations of the 2009 Racha earthquake, Georgia. Natural Hazards and Earth System Sciences, 2016, 16, 2137-2144. | 3.6 | 4 |
| 62 | Lava flow hazard at Fogo Volcano, Cabo Verde, before and after the 2014–2015 eruption. Natural Hazards and Earth System Sciences, 2016, 16, 1925-1951. | 3.6 | 69 |
| 63 | Secondary Fault Activity of the North Anatolian Fault near Avcilar, Southwest of Istanbul: Evidence from SAR Interferometry Observations. Remote Sensing, 2016, 8, 846. | 4.0 | 6 |
| 64 | Lithospheric flexure and gravity spreading of Olympus Mons volcano, Mars. Journal of Geophysical Research E: Planets, 2016, 121, 255-272. | 3.6 | 18 |
| 65 | Volcano dome dynamics at Mount St. Helens: Deformation and intermittent subsidence monitored by seismicity and camera imagery pixel offsets. Journal of Geophysical Research: Solid Earth, 2016, 121, 7882-7902. | 3.4 | 26 |
| 66 | Sentinel-1 tops interferometric time series results and validation. , 2016, , . | | 2 |
| 67 | Sloshing of a bubbly magma reservoir as a mechanism of triggered eruptions. Journal of Volcanology and Geothermal Research, 2016, 320, 156-171. | 2.1 | 32 |
| 68 | Gradual caldera collapse at Bárdarbunga volcano, Iceland, regulated by lateral magma outflow. Science, 2016, 353, aaf8988. | 12.6 | 230 |
| 69 | Rapid kinematic finite-fault inversion for an <i>M</i> _w 7+ scenario earthquake in the Marmara Sea: an uncertainty study. Geophysical Journal International, 2016, 204, 813-824. | 2.4 | 16 |
| 70 | Influence of volcanic tephra on photovoltaic (PV)-modules: an experimental study with application to the 2010 Eyjafjallajökull eruption, Iceland. Journal of Applied Volcanology, 2016, 5, . | 2.0 | 8 |
| 71 | Fault locking near Istanbul: indication of earthquake potential from InSAR and GPS observations. Geophysical Journal International, 2016, 205, 490-498. | 2.4 | 21 |
| 72 | The 2015 Gorkha earthquake investigated from radar satellites: slip and stress modeling along the MHT. Frontiers in Earth Science, 2015, 3, . | 1.8 | 24 |

| # | Article | IF | CITATIONS |
|----|---|-----|-----------|
| 73 | Sentinel-1 assessment of the interferometric wide-swath mode. , 2015, , . | | 14 |
| 74 | Insights into the 3D architecture of an active caldera ring-fault at Tendürek volcano through modeling of geodetic data. Earth and Planetary Science Letters, 2015, 422, 157-168. | 4.4 | 25 |
| 75 | Hydrothermal and magmatic reservoirs at Lazufre volcanic area, revealed by a high-resolution seismic noise tomography. Earth and Planetary Science Letters, 2015, 421, 27-38. | 4.4 | 34 |
| 76 | Triangular dislocation: an analytical, artefact-free solution. Geophysical Journal International, 2015, 201, 1119-1141. | 2.4 | 84 |
| 77 | Volcano-tectonic control of Merapi's lava dome splitting: The November 2013 fracture observed from high resolution TerraSAR-X data. Tectonophysics, 2015, 639, 23-33. | 2.2 | 47 |
| 78 | Satellite radar data reveal short-term pre-explosive displacements and a complex conduit system at VolcÃf¡n de Colima, Mexico. Frontiers in Earth Science, 2014, 2, . | 1.8 | 51 |
| 79 | Landslide observation and volume estimation in central Georgia based on L-band InSAR. Natural Hazards and Earth System Sciences, 2014, 14, 675-688. | 3.6 | 37 |
| 80 | The ring-shaped thermal field of Stefanos crater, Nisyros Island: a conceptual model. Solid Earth, 2014, 5, 183-198. | 2.8 | 15 |
| 81 | Deflation and inflation of a large magma body beneath Uturuncu volcano, Bolivia? Insights from InSAR data, surface lineaments and stress modelling. Geophysical Journal International, 2014, 198, 462-473. | 2.4 | 29 |
| 82 | Adaptive recognition and correction of baseline shifts from collocated GPS and accelerometer using two phases Kalman filter. Advances in Space Research, 2014, 54, 1924-1932. | 2.6 | 7 |
| 83 | Overlapping post-seismic deformation processes: afterslip and viscoelastic relaxation following the 2011 Mw 9.0 Tohoku (Japan) earthquake. Geophysical Journal International, 2014, 196, 218-229. | 2.4 | 85 |
| 84 | Application of a net-based baseline correction scheme to strong-motion records of the 2011 Mw 9.0 Tohoku earthquake. Geophysical Journal International, 2014, 197, 1808-1821. | 2.4 | 3 |
| 85 | A new algorithm for tight integration of real-time GPS and strong-motion records, demonstrated on simulated, experimental, and real seismic data. Journal of Seismology, 2014, 18, 151-161. | 1.3 | 27 |
| 86 | Directional flank spreading at Mount Cameroon volcano: Evidence from analogue modeling. Journal of Geophysical Research: Solid Earth, 2014, 119, 7542-7563. | 3.4 | 15 |
| 87 | Possible coupling of Campi Flegrei and Vesuvius as revealed by InSAR time series, correlation analysis and time dependent modeling. Journal of Volcanology and Geothermal Research, 2014, 280, 104-110. | 2.1 | 17 |
| 88 | Experimental study of the interplay between magmatic rift intrusion and flank instability with application to the 2001 Mount Etna eruption. Journal of Geophysical Research: Solid Earth, 2014, 119, 5356-5368. | 3.4 | 11 |
| 89 | Dome growth and coulée spreading controlled by surface morphology, as determined by pixel offsets in photographs of the 2006 Merapi eruption. Journal of Volcanology and Geothermal Research, 2013, 261, 121-129. | 2.1 | 37 |
| 90 | Aseismic deformation across the Hilina fault system, Hawaii, revealed by wavelet analysis of InSAR and GPS time series. Earth and Planetary Science Letters, 2013, 376, 12-19. | 4.4 | 26 |

| # | Article | IF | CITATIONS |
|-----|--|-----|-----------|
| 91 | Costâ€effective monitoring of ground motion related to earthquakes, landslides, or volcanic activity by joint use of a singleâ€frequency GPS and a MEMS accelerometer. Geophysical Research Letters, 2013, 40, 3825-3829. | 4.0 | 54 |
| 92 | Origins of obliqueâ€slip faulting during caldera subsidence. Journal of Geophysical Research: Solid Earth, 2013, 118, 1778-1794. | 3.4 | 42 |
| 93 | The 2011 Mw 9.0 Tohoku Earthquake: Comparison of GPS and Strong-Motion Data. Bulletin of the Seismological Society of America, 2013, 103, 1336-1347. | 2.3 | 134 |
| 94 | An active ring fault detected at Tendürek volcano by using InSAR. Journal of Geophysical Research: Solid Earth, 2013, 118, 4488-4502. | 3.4 | 18 |
| 95 | Coupling of Hawaiian volcanoes only during overpressure condition. Geophysical Research Letters, 2013, 40, 1994-1999. | 4.0 | 12 |
| 96 | Volcanic eruption monitoring by thermal image correlation: Pixel offsets show episodic dome growth of the Colima volcano. Journal of Geophysical Research: Solid Earth, 2013, 118, 1408-1419. | 3.4 | 35 |
| 97 | Comparison of InSAR two-pass and time series methods for analysing landslides in central Georgia, Caucasus. , 2012, , . | | 2 |
| 98 | Salt lake deformation detected from space. Earth and Planetary Science Letters, 2012, 331-332, 120-127. | 4.4 | 16 |
| 99 | Response of forearc crustal faults to the megathrust earthquake cycle: InSAR evidence from Mejillones Peninsula, Northern Chile. Earth and Planetary Science Letters, 2012, 333-334, 157-164. | 4.4 | 15 |
| 100 | Vertical and lateral collapse of Tharsis Tholus, Mars. Earth and Planetary Science Letters, 2011, 305, 445-455. | 4.4 | 23 |
| 101 | Low cost volcano deformation monitoring: optical strain measurement and application to Mount St. Helens data. Geophysical Journal International, 2011, 186, 699-705. | 2.4 | 39 |
| 102 | Comment on "The distribution of basaltic volcanism on Tenerife, Canary Islands: Implications on the origin and dynamics of the rift systems―by A. Geyer and J. MartÃ- Tectonophysics 483 (2010) 310–326. Tectonophysics, 2011, 503, 239-241. | 2.2 | 7 |
| 103 | Scale-dependent location of hydrothermal vents: Stress field models and infrared field observations on the Fossa Cone, Vulcano Island, Italy. Journal of Volcanology and Geothermal Research, 2011, 203, 133-145. | 2.1 | 40 |
| 104 | Estimating the Effect of Satellite Orbital Error Using Wavelet-Based Robust Regression Applied to InSAR Deformation Data. IEEE Transactions on Geoscience and Remote Sensing, 2011, 49, 4600-4605. | 6.3 | 65 |
| 105 | Structural architecture of the 1980 Mount St. Helens collapse: An analysis of the Rosenquist photo sequence using digital image correlation. Geology, 2011, 39, 767-770. | 4.4 | 15 |
| 106 | Gravity-driven deformation of Damavand volcano, Iran, detected through InSAR time series. Geology, 2011, 39, 251-254. | 4.4 | 15 |
| 107 | Propagation, linkage, and interaction of caldera ring-faults: comparison between analogue experiments and caldera collapse at Miyakejima, Japan, in 2000. Bulletin of Volcanology, 2010, 72, 297-308. | 3.0 | 35 |
| 108 | Subduction earthquake deformation associated with 14 November 2007, Mw 7.8 Tocopilla earthquake in Chile: Results from InSAR and aftershocks. Tectonophysics, 2010, 490, 60-68. | 2.2 | 49 |

| # | Article | IF | CITATIONS |
|-----|---|------|-----------|
| 109 | Relationship between the InSAR-measured uplift, the structural framework, and the present-day stress field at Lazufre volcanic area, central Andes. Tectonophysics, 2010, 492, 133-140. | 2.2 | 28 |
| 110 | On the effects of 3â€Ð mechanical heterogeneities at Campi Flegrei caldera, southern Italy. Journal of Geophysical Research, 2010, 115, . | 3.3 | 47 |
| 111 | Satellite Monitoring of Hazards: A Focus on Istanbul, Turkey. Eos, 2010, 91, 313-314. | 0.1 | 10 |
| 112 | Timeâ€dependent volcano source monitoring using interferometric synthetic aperture radar time series: A combined genetic algorithm and Kalman filter approach. Journal of Geophysical Research, 2010, 115, . | 3.3 | 24 |
| 113 | L-band and C-band InSAR studies of African volcanic areas. , 2009, , . | | 4 |
| 114 | Volcano spreading and fault interaction influenced by rift zone intrusions: Insights from analogue experiments analyzed with digital image correlation technique. Journal of Volcanology and Geothermal Research, 2009, 183, 170-182. | 2.1 | 40 |
| 115 | Surface deformation time series and source modeling for a volcanic complex system based on satellite wide swath and image mode interferometry: The Lazufre system, central Andes. Remote Sensing of Environment, 2009, 113, 2062-2075. | 11.0 | 41 |
| 116 | Volcanic activity before and after large tectonic earthquakes: Observations and statistical significance. Tectonophysics, 2009, 471, 14-26. | 2.2 | 87 |
| 117 | Structural features of Panarea volcano in the frame of the Aeolian Arc (Italy): Implications for the 2002–2003 unrest. Journal of Geodynamics, 2009, 47, 288-292. | 1.6 | 10 |
| 118 | Volcanic and geochemical evolution of the Teno massif, Tenerife, Canary Islands: Some repercussions of giant landslides on ocean island magmatism. Geochemistry, Geophysics, Geosystems, 2009, 10, . | 2.5 | 47 |
| 119 | Randomly iterated search and statistical competency as powerful inversion tools for deformation source modeling: Application to volcano interferometric synthetic aperture radar data. Journal of Geophysical Research, 2009, 114, . | 3.3 | 32 |
| 120 | Stress transfer in the Lazufre volcanic area, central Andes. Geophysical Research Letters, 2009, 36, . | 4.0 | 36 |
| 121 | Simultaneous magma and gas eruptions at three volcanoes in southern Italy: An earthquake trigger?. Geology, 2009, 37, 251-254. | 4.4 | 50 |
| 122 | The effects of flank collapses on volcano plumbing systems. Geology, 2009, 37, 1099-1102. | 4.4 | 93 |
| 123 | Land subsidence pattern controlled by old alpine basement faults in the Kashmar Valley, northeast Iran: results from InSAR and levelling. Geophysical Journal International, 2008, 174, 287-294. | 2.4 | 33 |
| 124 | Coseismic slip model of the 2007 August Pisco earthquake (Peru) as constrained by Wide Swath radar observations. Geophysical Journal International, 2008, 174, 842-848. | 2.4 | 33 |
| 125 | Caldera-scale inflation of the Lazufre volcanic area, South America: Evidence from InSAR. Journal of Volcanology and Geothermal Research, 2008, 174, 337-344. | 2.1 | 39 |
| 126 | Low-temperature hydrothermal alteration of intra-caldera tuffs, Miocene Tejeda caldera, Gran Canaria, Canary Islands. Journal of Volcanology and Geothermal Research, 2008, 176, 551-564. | 2.1 | 36 |

| # | Article | IF | CITATIONS |
|-----|---|------|-----------|
| 127 | The 26 May 2006 magnitude 6.4 Yogyakarta earthquake south of Mt. Merapi volcano: Did lahar deposits amplify ground shaking and thus lead to the disaster?. Geochemistry, Geophysics, Geosystems, 2008, 9, . | 2.5 | 51 |
| 128 | Land subsidence in Iran caused by widespread water reservoir overexploitation. Geophysical Research Letters, 2008, 35, . | 4.0 | 191 |
| 129 | InSAR time series investigation of land subsidence due to groundwater overexploitation in Tehran, Iran. , 2008, , . | | 7 |
| 130 | Chapter 9 Facilitating Dike Intrusions into Ring-Faults. Developments in Volcanology, 2008, 10, 351-374. | 0.5 | 6 |
| 131 | Influences of magma chamber ellipticity on ring fracturing and eruption at collapse calderas. IOP Conference Series: Earth and Environmental Science, 2008, 3, 012018. | 0.3 | 0 |
| 132 | Unzipping Long Valley: An explanation for vent migration patterns during an elliptical ring fracture eruption. Geology, 2008, 36, 323. | 4.4 | 29 |
| 133 | Volcanic eruptions following M ≥ 9 megathrust earthquakes: Implications for the Sumatra-Andaman volcanoes. Geology, 2007, 35, 539. | 4.4 | 164 |
| 134 | How a tectonic earthquake may wake up volcanoes: Stress transfer during the 1996 earthquake–eruption sequence at the Karymsky Volcanic Group, Kamchatka. Earth and Planetary Science Letters, 2007, 264, 347-359. | 4.4 | 73 |
| 135 | Stress Control of Deep Rift Intrusion at Mauna Loa Volcano, Hawaii. Science, 2007, 316, 1026-1030. | 12.6 | 91 |
| 136 | Volcanic activity influenced by tectonic earthquakes: Static and dynamic stress triggering at Mt. Merapi. Geophysical Research Letters, 2007, 34, . | 4.0 | 106 |
| 137 | Soft volcanic sediments compound 2006 Java earthquake disaster. Eos, 2007, 88, 486-486. | 0.1 | 4 |
| 138 | Land subsidence in Mashhad Valley, northeast Iran: results from InSAR, levelling and GPS. Geophysical Journal International, 2007, 168, 518-526. | 2.4 | 143 |
| 139 | Effects of mechanical layering on volcano deformation. Geophysical Journal International, 2007, 170, 952-958. | 2.4 | 82 |
| 140 | Volcano-earthquake interaction at Mauna Loa volcano, Hawaii. Journal of Geophysical Research, 2006, 111, n/a-n/a. | 3.3 | 57 |
| 141 | Gravitational spreading and formation of new rift zones on overlapping volcanoes. Terra Nova, 2006, 18, 26-33. | 2.1 | 35 |
| 142 | Gravitational spreading controls rift zones and flank instability on El Hierro, Canary Islands. Geological Magazine, 2006, 143, 257-268. | 1.5 | 44 |
| 143 | Unveiling the origin of radial grabens on Alba Patera volcano by finite element modelling. Icarus, 2005, 176, 44-56. | 2.5 | 22 |
| 144 | Elliptical calderas in active tectonic settings: an experimental approach. Journal of Volcanology and Geothermal Research, 2005, 144, 119-136. | 2.1 | 98 |

| # | Article | IF | CITATIONS |
|-----|--|----------|--------------|
| 145 | Rift zone reorganization through flank instability in ocean island volcanoes: an example from Tenerife, Canary Islands. Bulletin of Volcanology, 2005, 67, 281-291. | 3.0 | 86 |
| 146 | Large-scale failures on domes and stratocones situated on caldera ring faults: sand-box modeling of natural examples from Kamchatka, Russia. Bulletin of Volcanology, 2005, 67, 457-468. | 3.0 | 25 |
| 147 | Gravitational spreading causes en-echelon diking along a rift zone of Madeira Archipelago: an experimental approach and implications for magma transport. Bulletin of Volcanology, 2005, 68, 37-46. | 3.0 | 34 |
| 148 | Feedback processes between magmatic events and flank movement at Mount Etna (Italy) during the 2002–2003 eruption. Journal of Geophysical Research, 2005, 110, . | 3.3 | 107 |
| 149 | Influence of volcanic activity at Mauna Loa, Hawaii, on earthquake occurrence in the Kaoiki Seismic Zone. Geophysical Research Letters, 2004, 31, n/a-n/a. | 4.0 | 17 |
| 150 | Experiments on rift zone evolution in unstable volcanic edifices. Journal of Volcanology and Geothermal Research, 2003, 127, 107-120. | 2.1 | 91 |
| 151 | Buttressing and fractional spreading of Tenerife, an experimental approach on the formation of rift zones. Geophysical Research Letters, 2003, 30, . | 4.0 | 36 |
| 152 | Modeling volcanic deformation in a regional stress field: Implications for the formation of graben structures on Alba Patera, Mars. Journal of Geophysical Research, 2003, 108, . | 3.3 | 39 |
| 153 | HMG-CoA Reductase Inhibitors Are Associated with Decreased Serum Neopterin Levels in Stable Coronary Artery Disease. Clinical Chemistry and Laboratory Medicine, 2003, 41, 1314-9. | 2.3 | 27 |
| 154 | Cyclic caldera collapse: Piston or piecemeal subsidence? Field and experimental evidence. Geology, 2002, 30, 135. | 4.4 | 91 |
| 155 | Shape and structure of (analogue models of) refolded layers. Journal of Structural Geology, 2002, 24, 1313-1326. | 2.3 | 29 |
| 156 | Rifting, recurrent landsliding and Miocene structural reorganization on NW-Tenerife (Canary) Tj ETQq0 0 0 rgBT | Overlock | 10 Tf 50 302 |

| 157 | Formation of caldera periphery faults: an experimental study. Bulletin of Volcanology, 2001, 63, 191-203. | 3.0 | 164 |
|-----|--|------|-----|
| 158 | Thermal UAS survey of reactivated hot spring activity in Waiwera, New Zealand. Advances in Geosciences, 0, 54, 165-171. | 12.0 | 4 |